Title

Inhibition of soluble epoxide hydrolase attenuates hepatic fibrosis and endoplasmic reticulum stress induced by carbon tetrachloride in mice

Journal

Toxicology and Applied Pharmacology, 286(2)

ISSN

0041-008X

Authors

Harris, Todd R
Bettaieb, Ahmed
Kodani, Sean
et al.

Publication Date

2015-07-01

DOI

10.1016/j.taap.2015.03.022

Peer reviewed

HHS Public Access

Author manuscript

Toxicol Appl Pharmacol. Author manuscript; available in PMC 2016 July 15.

Published in final edited form as:

Toxicol Appl Pharmacol. 2015 July 15; 286(2): 102–111. doi:10.1016/j.taap.2015.03.022.

Inhibition of soluble epoxide hydrolase attenuates hepatic fibrosis and endoplasmic reticulum stress induced by carbon tetrachloride in mice

Todd R. Harris[*], **Ahmed Bettaieb**[†], **Sean Kodani**[*], **Hua Dong**[*], **Richard Myers**[‡], **Nipavan Chiamvimonvat**[‡], **Fawaz G. Haj**[†,^], and **Bruce D. Hammock**[*,§]

[*]Department of Entomology and Comprehensive Cancer Center, University of California, Davis, CA 95616, USA

[†]Department of Nutrition, University of California, Davis, CA 95616, USA

[‡]Department of Internal Medicine: Cardiovascular, University of California, Davis, CA 95616, USA

[^]Department of Internal Medicine: Endocrinology, Diabetes and Metabolism, University of California, Davis, CA 95616, USA

Abstract

Liver fibrosis is a pathological condition in which chronic inflammation and changes to the extracellular matrix lead to alterations in hepatic tissue architecture and functional degradation of the liver. Inhibitors of the enzyme soluble epoxide hydrolase (sEH) reduce fibrosis in the heart, pancreas and kidney in several disease models. In this study, we assess the effect of sEH inhibition on the development of fibrosis in a carbon tetrachloride (CCl_4)-induced mouse model by monitoring changes in the inflammatory response, matrix remolding and endoplasmic reticulum stress. The sEH inhibitor 1-trifluoromethoxyphenyl-3-(1-propionylpiperidin-4-yl) urea (TPPU) was administered in drinking water. Collagen deposition in the liver was increased five-fold in the CCl_4-treated group, and this was returned to control levels by TPPU treatment. Hepatic expression of Col1a2 and 3a1 mRNA was increased over fifteen-fold in the CCl_4-treated group relative to the control group, and this increase was reduced by 50% by TPPU treatment. Endoplasmic reticulum (ER) stress observed in the livers of CCl_4-treated animals was attenuated by TPPU treatment. In order to support the hypothesis that TPPU is acting to reduce the hepatic fibrosis and ER stress through its action as a sEH inhibitor we used a second sEH inhibitor, *trans*-4-{4-[3-(4-trifluoromethoxy-phenyl)-ureido]-cyclohexyloxy}-benzoic acid (*t*-TUCB), and sEH null mice. Taken together, these data indicate that the sEH may play an important role in the development of

[§]Corresponding Author: Bruce D. Hammock, Department of Entomology and Comprehensive Cancer Center, University of California, Davis, 1 Shields Avenue, Davis, CA 95616, USA, tele: (530) 752 7519, bdhammock@ucdavis.edu.

Conflict of Interest

B.D.H. is a co-founder of EicOsis LLC and has several patents on soluble epoxide hydrolase technology. The remaining authors have nothing to disclose.

hepatic fibrosis induced by CCl_4, presumably by reducing endogenous fatty acid epoxide chemical mediators acting to reduce ER stress.

Keywords

soluble epoxide hydrolase; endoplasmic reticulum stress; carbon tetrachloride; fibrosis

Introduction

Liver fibrosis is a pathological condition that results from a normally beneficial wound healing process (Hernandez-Gea and Friedman, 2011). Damage to the liver triggers the inflammatory response, which initiates recruitment of macrophages and fibrocytes and remodeling of the extracellular matrix (ECM) in order to clear damaged cells and preserve the architecture of the liver (Bataller and Brenner, 2005). However, repeated injury, such as occurs in chronic alcoholism, exposure to environmental toxins, and viral infection can lead to a cascade of inflammatory system-related changes in the liver that result in abnormal deposition and composition of collagens and other elements of the ECM, as well as extensive damage to the tissue (Iredale, 2007). This pathological condition is called fibrosis.

Fibrosis is facilitated by a number of signaling molecules that modulate the immune response such as the cytokines IL-6 and IL-1β and the growth factor TGFβ (Wynn and Ramalingam, 2012). Alongside these commonly studied protein inflammatory mediators, bioactive lipids play an important role (Funk, 2001; Stables and Gilroy, 2011). There is growing evidence of the importance of lipid signaling in liver fibrosis. The eicosanoids are a class of lipid mediators that includes the leukotrienes, prostaglandins and epoxyeicosatrienoic acids (EETs), produced through the activity of lipoxygenase (LOX), cyclooxygenase (COX) and cytochrome P450 enzymes, respectively (Funk, 2001; Stables and Gilroy, 2011). The leukotrienes and prostaglandins have been implicated in the progression of liver fibrosis in studies employing leukotriene receptor antagonists and COX inhibitors. A leukotriene receptor antagonist, montelukast, attenuates liver damage and fibrosis in a bile duct ligation (BDL) and resection rat model (El-Swefy and Hassanen, 2009). A COX inhibitor, meloxicam, reduces fibrosis in this same model (Kim *et al.*, 2008), although contradictory results have been reported using celecoxib (Yu *et al.*, 2009).

A third class of arachidonic acid-derived mediators, the EETs, display anti-inflammatory and anti-fibrotic properties (Stables and Gilroy, 2011). The EETs are metabolized by soluble epoxide hydrolase (sEH), producing dihydroxy molecules that are less lipophilic and more readily conjugated, leading to their removal from the site of action (Morisseau and Hammock, 2013). sEH inhibitors modulate the levels of epoxy fatty acids (EpFAs) in tissues and dramatically reduce acute systemic inflammation in LPS-induced models as well as attenuate fibrosis and inflammation in the heart, kidney and pancreas (Li *et al.*, 2008; Iyer *et al.*, 2012; Kompa *et al.*, 2013; Sirish *et al.*, 2013). In diabetic models, sEH inhibitors display organ protective properties, reducing islet cell apoptosis in the pancreas and tissue damage in the liver (Iyer *et al.*, 2012). It has been hypothesized that these inhibitors act by blocking the major route of metabolism of organ protective and anti-inflammatory EpFA (Iyer *et al.*,

2012). Given these reported findings, we evaluated a sEH inhibitor in a murine model of liver fibrosis.

Once activated by metabolism, carbon tetrachloride (CCl_4) causes damage to the liver through lipid peroxidation, resulting in an upregulation of pro-inflammatory pathways and eventual fibrosis (Iredale, 2007). EpFA have been implicated in this model. Both COX-2 and 5-LOX inhibitors have been found to reduce fibrosis after CCl_4 treatment, and when used in combination, reduce both inflammation and necrosis (Horrillo *et al.*, 2007), though there are contradictory results when different COX-2 inhibitors are employed, as in the BDL model of fibrosis (Hui *et al.*, 2006). Dietary supplementation with arachidonic acid and the omega-3 docosahexaenoic acid (DHA) has been found to attenuate fibrosis in an ethanol-induced model of liver damage (Song *et al.*, 2008).

A growing body of evidence indicates that endoplasmic reticulum (ER) stress is a contributor to fibrotic diseases (Mollica *et al.*, 2011; Lenna and Trojanowska, 2012; Tanjore *et al.*, 2012). Directly relevant to this study, recent reports have demonstrated an increase in ER stress in rodents injected with CCl_4 (Ji *et al.*, 2011; Lee *et al.*, 2011; Jin *et al.*, 2013). However, the link between the development of hepatic fibrosis and ER stress is still poorly understood. The ER is highly responsive to nutrients and to the energy state of the cell. It plays an important role in folding of newly synthesized proteins. When the folding capacity of the ER is exceeded, misfolded proteins accumulate and lead to ER stress (Schroder and Kaufman, 2005). Cells use adaptive mechanisms to counter the deleterious effects of ER stress known as the unfolded protein response (Kaufman *et al.*, 2002). The unfolded protein response consists of three major branches that are controlled by the ER transmembrane proteins PKR-like ER-regulated kinase (PERK), inositol requiring protein 1α (IRE1α), and activating transcription factor 6 (ATF6) (Hotamisligil; Hummasti and Hotamisligil; Ron and Walter, 2007). In particular, the IRE1α sub-arm of ER stress signaling is critical for the unfolded protein response in fibrotic tissues (Chiang *et al.*, 2011; Martino *et al.*, 2013). The various unfolded protein response sub-arms synergize to attenuate stress by increasing the folding capacity of the ER (Schroder and Kaufman, 2005). However, if the compensatory mechanisms fail to facilitate the adaptation of cells to ER stress, induction of the unfolded protein response can lead to elimination of stressed cells by apoptosis (Zinszner *et al.*, 1998; Nishitoh *et al.*, 2002). We recently demonstrated that sEH deficiency or pharmacological inhibition in mice attenuated chronic high fat diet-induced ER stress in liver and adipose tissue in a cell autonomous manner (Bettaieb *et al.*, 2013).

Based on the above information we examined markers of ER stress in our murine model of liver fibrosis and asked if they could be reduced by treatment with sEH inhibitors.

Materials and Methods

Reagents

TPPU (1-trifluoromethoxyphenyl-3-(1-propionylpiperidin-4-yl) urea) (Rose *et al.*, 2010) and *t*-TUCB (*trans*-4-{4-[3-(4-trifluoromethoxy-phenyl)-ureido]-cyclohexyloxy}-benzoic acid), (Hwang et al., 2007) were synthesized and the physical properties assessed as previously reported. Antibodies for pPERK (Thr980), PERK, peIF2α (Ser51), eIF2α, sXBP1, ATF6,

IRE1α, and BiP were purchased from Santa Cruz Biotechnology (Santa Cruz, CA) while phospho-p38 (Thr180/Tyr182), p38, pJNK (Thr183/Tyr185), JNK and cleaved Caspase3 antibodies were from Cell Signaling (Beverly, MA). Antibodies for pIRE1α (Ser724) were purchased from Abcam (Cambridge, MA). Horseradish peroxidase (HRP)-conjugated secondary antibodies were purchased from BioResources International (Carlsbad, CA). Unless otherwise indicated, all other chemicals were purchased from Sigma (St. Louis, MO).

Animals

All animal studies were approved by the University of California Davis Animal Use and Care Committee and were performed in accordance with the National Institutes of Health guide for the care and use of laboratory animals. Male C57BL (20g) were obtained from Charles River Laboratories (Wilmington, MA). A colony of C57BL mice with a disruption in the sEH gene resulting in a functional knockout is maintained by the UC Davis Mouse Biology Program (Luria *et al.*, 2007). Mice were divided into four groups of 8: The Control group was given interperiotineal injections (I.P.) of sterile filtered Neobee M-5 (Fisher Scientific, Houston, TX) every five days for five weeks, for a total of 7 injections. They also received drinking water containing 1% PEG-400 (Fisher Scientific). The CCl_4-only group was given I.P. injections of 197 mg/kg CCl_4 (Sigma) mixed 1:7 in sterile filtered Neobee M-5 every five days for five weeks, for a total of 7 injections. This dose and route of administration was chosen since it has been shown to induce robust fibrosis in C57BL mice (Constandinou, *et al*. 2005). They received drinking water containing 1% PEG-400 (Fisher Scientific). The CCl_4+TPPU group was treated with CCl_4 similar to the CCl_4-only group and received drinking water with 10 mg/L TPPU and 1% PEG-400, prepared as follows. TPPU was dissolved in PEG-400 to give a 1000 mg/L clear solution. This solution was then added to warm drinking water with rapid stirring to give the 10 mg/L solution of TPPU in 1% PEG-400 in drinking water. The water was provided ad lib. The TPPU-only group was given I.P. injections of sterile filtered Neobee M-5 like the Control group, and received drinking water containing TPPU similar to the CCl_4+inhibitor groups. In the experiment with the second sEH inhibitor, *t*-TUCB was solubilized in PEG-400 and then added to drinking water, resulting in a final concentration 10 mg/L TPPU and 1% PEG-400. Based on estimated of daily water consumption, a concentration of 10 mg/L inhibitor in drinking water will result in a dose of approximately 1.7 mg/kg/day. The mice were sacrificed three days after the final injection.

Histology

Liver samples were embedded, sectioned and stained by the UC Davis Veterinary Medical Teaching Hospital Anatomic Pathology Service (Davis, CA). The slides were imaged using a Nikon Diaphot inverted microscope and quantified using ImageJ (NIH, Bethesda, MD).

Protein Analysis

Mouse tissues were dissected and immediately frozen in liquid nitrogen. For zymography, liver samples were homogenized in cold 25 mM Tris-HCl buffer using 3 × 30 s bursts of a roto-stator homogenizer with one minute intervals in between. Zymography was performed

using Novagen pre-cast gelatin zymography gels (Invitrogen, Carlsbad, CA) according to manufacturer's instructions and quantified using ImageJ (NIH). For Western blots, tissues were ground in the presence of liquid nitrogen and lysed using radio-immunoprecipitation assay (RIPA) buffer (10 mM Tris-HCl, pH 7.4, 150 mM NaCl, 0.1% sodium dodecyl sulfate [SDS], 1% Triton X-100, 1% sodium deoxycholate, 5 mM EDTA, 1 mM NaF, 1 mM sodium orthovanadate and protease inhibitors). Lysates were clarified by centrifugation at 10,000 × g for 10 min and protein concentrations were determined using a bicinchoninic acid protein assay kit (Thermo Scientific, Waltham, MA). Proteins were resolved by SDS-PAGE and transferred to PVDF membranes. Immunoblots were performed with the relevant antibodies. Proteins were visualized using Luminata™ Forte (Millipore, Billerica, MA). For quantitation purposes, pixel intensities of immuno-reactive bands from blots that were in the linear range of loading and exposure were quantified using FluorChem 9900 (Alpha Innotech, San Lenardo, CA).

Quantitative real time PCR

Fresh liver samples were immersed in RNALater (Qiagen, Carol Stream, IL) and left at 4° C overnight before storage at −80° C. Liver tissue was homogenized by roto-stator in a single 45 s burst and the lysates were passed through a QIAshredder column according to manufacturer's suggestion (Qiagen). Total RNA was isolated using the RNeasy miniprep kit (Qiagen) and first strand cDNA synthesized using the RT^2 First Strand Kit (Qiagen). Gene expression was assessed by the RT^2 Profiler PCR Array (Mouse Fibrosis) for ABI 7500 Fast Block (Invitrogen). For qRT-PCR mRNA of BiP, sXBP1, ATF4, ATF6 and CHOP was assessed by reverse transcription PCR (iCycler, BioRad, Hercules, CA) and normalized to TATA-Box binding protein. For RT-PCR, Absolute blue qPCR premix (Fisher Scientific) was mixed with each primer. ATF4 primers: : 5′-GACCTGGAAACCATGCCAGA -3′ (For.), 5′-TGGCCAATTGGGTT CACTGT -3′ (Rev.); ATF6 primers: 5′-TGTATTACGCCTCCCCTGGA -3′ (For.), 5′-ACACAGCAGAACCAACACCA -3′ (Rev.); CHOP primers: 5′-CCCTGCCTTTCACCTTGG -3′ (For.), 5′-CCGCTCGTTCTCCTGCTC -3′ (Rev.); BiP primers: 5′-ACTTGGGGACCACCTATTCCT -3′ (For.), 5′-ATCGCCAATCAGACGCTCC -3′ (Rev.); sXBP-1 primers: 5′-GGTCTGCTGAGTCCGCAGCAGG -3′ (For.), 5′-AGGCTTGGTGTATA CATGG -3′ (Rev.); TATA binding protein primers: 5′-TTGGCTAGGTTTCTGCG GTC -3′ (For.), 5′-TGCTGTAGCCGTATTCATTG -3′ (Rev.).

LC-MS/MS analysis of plasma oxylipins

Plasma oxylipins were extracted and analyzed by LC-MS/MS as previously described (Yang *et al.*, 2009). Blood levels of inhibitors were determined by LC-MS/MS as previously described (Liu *et al.*, 2013). Retention time, selected reaction monitoring and internal standard information used to quantify all analytes in supplementary materials Table S1.

LC-MS/MS analysis of hydroxyproline

The quantification of hepatic tissue hydroxyproline by LC-MS/MS was performed using the method developed by Kindt *et al* (2003) with the following changes. The analysis was carried out using a Micromass Quattro Ultima triple quadrupole tandem mass spectrometer

(Micromass, Manchester, UK) equipped with an electrospray ionization interface. The HPLC system consisted of a Waters model 2790 separations module (Waters, Milford, MA) equipped with a Waters model 2487 dual-wavelength absorbance detector. The mass spectrometer was coupled to the outlet of the HPLC (Pursuit C18, 2.0 × 150 mm, 3 μm column (Agilent, Englewood, CO)).

Statistical analysis

All data are expressed as mean ± standard error. The Student's *t*-test was used to test for differences in groups in all experiments. Statistical analyses were performed using Excel (Microsoft, Redmond, WA). Differences were considered significant with P-value < 0.05 or lower. Sample size "N" refers to the number of animals.

Results

Administration of the sEH inhibitor TPPU reduced CCl_4-induced collagen deposition and collagen mRNA expression

Animals were treated with CCl_4 for five weeks to induce liver fibrosis. To potentially reduce development of this fibrosis, the sEH inhibitor TPPU was chosen due to its potency on and selectivity for the sEH target and because of its ADME properties in mice (Liu *et al.*, 2013). TPPU was administered in drinking water starting with the first CCl_4 injection, and blood levels of the compound were assessed at 2.5 weeks and at the termination of the experiment. At both time points, taken at 8 AM from mice on a 7 AM to 7 PM light cycle, the TPPU-treated concentration of the inhibitor was approximately 500 nM (2.5 wk = 511 ± 37 nM, 5 wk = 543 ± 17 nM). All experimental groups gained weight during the six week experiment (supplementary materials). The CCl_4-only and TPPU-only groups displayed a greater weight gain than the CCl_4+TPPU and Control groups. Three days after the last injection of CCl_4, the livers were removed and prepared for protein, mRNA, and histological analysis. Sections were stained with picosirius red (Figure 1A).

The percent area stained by picosirius red relative to the Control group increased five-fold in the CCl_4-only group, while the CCl_4+TPPU group returned to the level of the Control group (Figure 1B). The CCl_4-only group displayed a roughly six-fold increase in total hepatic tissue hydroxyproline as determined by LC-MS/MS (Figure 1C). The CCl_4+TPPU group was not statistically different (P-value > 0.05) from either the Control or the CCl_4-only groups (Figure 1C). Staining for alpha smooth muscle actin (α-SMA) revealed an increase in percent area stained in the CCl_4-only group relative to the Control group that was not significantly altered by TPPU treatment (supplementary materials Figure S2). A PCR array experiment (described in detail below) determined that the messages for collagens 1a2 and 3a1 were upregulated approximately sixteen fold in the CCl_4-only group (Figure 3). The upregulation was reduced by 50% in the CCl_4 +TPPU group. This indicates that TPPU treatment has an effect on both the expression and deposition of collagen due to CCl_4 treatment.

Administration of the sEH inhibitor TPPU modulated the mRNA expression and activity of MMPs and the mRNA expression of other components of the ECM

In order to assess the signaling pathways involved in the anti-fibrotic effect of TPPU treatment, a PCR array was run that included growth factors, cytokines, chemokines and components of the ECM involved in the progression of fibrosis. When compared to the Control group, the CCl_4-only group displayed 33 genes upregulated 1.5 fold or more with a P-value of 0.5 or lower (Figure 2). The CCl_4 +TPPU group displayed 20 genes upregulated 1.5 fold or more with a P-value of 0.5 or lower compared to the Control group (Figure 2). The thirteen genes that differentiated the CCl_4-only and CCl_4+TPPU groups with a P-value of 0.5 or lower are displayed in Figure 3. To validate these results, the mRNA expression of three genes included in the array were independently determined by RTPCR and found to display the same trend as reported by the array (supplementary materials Table S3). Compared to the CCl_4-only group, the CCl_4+TPPU group displayed a decrease in mRNA expression of MMP-2, -8, -9, -13, and -14 (Figure 3). The largest reduction occurring for MMP-8 and MMP-9, which were decreased approximately four-fold from the CCl_4-only group. MMP-1a was increased by approximately two-fold in the CCl_4-only and CCl_4+TPPU groups compared to control (supplementary materials Table S2). Of the Tissue Inhibitors of Metalloproteases (TIMPs), only TIMP-2 showed a statistically significant (P-value < 0.05) modulation in the CCl_4-only group relative to the Control group (supplementary materials Table S2). In the CCl_4-only and CCL_4+TPPU groups, TIMP-2 expression was upregulated 3.5 and 2.5 fold, respectively. The modulation of the expression of several MMPs prompted us to examine MMP activity in the hepatic tissues. Using a randomly selected subset of samples from the experimental groups, we performed gelatin zymography, which assays MMP-1, -2 and -9 activity, primarily (Snoek-van Beurden and Von den Hoff, 2005). Intracellular pools of MMP-1a, -2, and -9 contain both pro- and active- forms of the enzymes, the active form produced when a roughly 10 kDa peptide is cleaved from the pro-form. In zymography, the enzymes are separated by native PAGE and then both forms the enzymes activated. We detected an increase in gelatinase activity in the CCl_4-only group in the 90–107 kDa range relative to the Control group, which spans the molecular weight of the 92 kDa pro-MMP-9 (Figure 4). This activity was reduced in the CCl_4+TPPU group. We also detected a large increase in gelatinase activity in the 45–54 kDa range in the CCl_4+TPPU group relative to the Control group, corresponding to the molecular weight of active MMP-1a, which has a roughly 57 kDa pro-form and a 48 kDa active form (Balbin *et al.*, 2001). This activity was only slightly increased in the CCl_4-only group. We also detected a moderate increase in gelatinase activity in the 62–69 kDa molecular weight range in the CCl_4-only and CCl_4+TPPU groups, corresponding to active MMP-2, which is roughly 62 kDa (supplementary materials Figure S3).

TPPU treatment significantly modulated the mRNA expression of two other components of the ECM, integrin α2 (Itgα2) and Thrombspondin 2. The three-fold induction in Itgα2 between the CCl_4-only and Control group was reduced by almost 50% in CCl_4+TPPU group (Figure 3). Thrombspondin 2 was increased almost six-fold in CCl_4-only group relative to the Control group. This increase was attenuated by 33% in CCl_4+TPPU group (Figure 3).

Administration of TPPU modulated the inflammatory response

Of the chemokines and chemokine receptors in the PCR array, two receptors, C–C chemokine receptor 2 and C-X-C motif chemokine receptor-4 were significantly reduced in the CCl_4+TPPU group relative to the CCl_4-only group (Figure 3). C–C chemokine receptor 2 was increased over five-fold in the CCl_4-only group relative to the Control group, and this increase was almost halved in the CCl_4+TPPU group. Similarly, an over 4-fold increase in C-X-C motif chemokine receptor-4 mRNA expression in the CCl_4-only group relative to the Control group was reduced by 50% in the CCl_4+TPPU group. The PCR array also revealed that an almost 2 fold increase in TGFβ1 in the CCl_4-only group relative to the Control group was decreased to control level in the CCl_4+TPPU group (Figure 3).

Since sEH inhibitors have been shown to modulate the inflammatory EpFA in other disease models, we examined blood levels of oxylipids (supplementary materials Table S4, Figures S4, and S5). We did not see a statistically significant difference in most classes, including the EETs. However, one lipid mediator, the 12-LOX metabolite 12-HETE, was increased over 3-fold in the CCl_4 group. Levels of this EpFA were reduced in the CCl_4+TPPU group, but did not reach statistical significance.

Administration of TPPU attenuated CCl_4-induced ER stress

ER stress is an emerging factor in fibrotic diseases and a number of studies have identified significant correlation between hepatic fibrosis and ER stress (Mollica *et al.*, 2011; Lenna and Trojanowska, 2012; Tanjore *et al.*, 2012), although the precise mechanism is not clear. In this study we investigated whether exposure to CCl_4 induces hepatic ER stress *in vivo* and evaluated the effects of sEH pharmacological inhibition on CCl_4-induced hepatic ER stress. In line with published studies exposure to CCl_4 induced ER stress (Lewis and Roberts, 2005; Lee *et al.*, 2011; Jin *et al.*, 2013), as evidenced by increased PERK (Thr^{980}), eIF2α (Ser^{51}) and IRE1α (Ser^{724}) phosphorylation and increased sXBP1 expression in liver lysates (Figure 5A). Importantly, pharmacological inhibition of sEH attenuated hepatic ER stress in CCl_4-treated mice as evidenced by decreased PERK (Thr^{980}), eIF2α (Ser^{51}) and IRE1α (Ser^{724}) phosphorylation and decreased sXBP1 expression (Figure 5A). In line with these findings, hepatic mRNA of BiP, sXBP1 ATF4, ATF6 and CHOP was decreased upon pharmacological inhibition of sEH compared with CCl_4-treated mice, indicating attenuated ER stress (Figure 5B).

Excessive ER stress leads to the induction of inflammatory responses and eventually cell death (Zha and Zhou). In addition, CCl_4-induced liver injury has been shown to involve TNF-α-and TGF-β-mediated activation of JNK and cell death (Hong *et al.*, 2013; Ma *et al.*, 2013; Wu and Cederbaum, 2013). Thus, we investigated the effects of pharmacological inhibition of sEH on CCl_4-induced inflammation. Consistent with previous reports, induction of liver fibrosis correlated with increased hepatic JNK and p38 phosphorylation (Figure 5C). On the other hand, sEH pharmacological inhibition reduced CCl_4-induced phosphorylation of JNK and p38 (Figure 5C). After exposure to apoptotic stimuli, cells activate initiator caspases that proteolytically cleave and activate effector caspases (such as caspase-3) to dismantle the dying cell. Caspase3 is implicated in ER stress-induced cell death (Zhang *et al.*; Zhang *et al.*). Accordingly, we determined ER stress-induced expression

of active caspase-3 in CCl_4-treated mice versus mice with combined treatment (CCl_4+TPPU). Consistent with published reports (Chan *et al.*, 2013; Moran-Salvador *et al.*, 2013), treatment with CCl_4 caused a significant increase in the expression of the active form of caspase3 whereas sEH inhibition significantly decreased CCl_4-induced caspase-3 activation (Figure 5D). Together, these results indicate that the pharmacological inhibition of sEH can provide a protective mechanism against CCl_4-induced ER stress in the liver.

Disruption of the sEH gene or administration of an alternate sEH inhibitor reduced collagen deposition

In order to support the hypothesis that TPPU is acting to reduce the hepatic fibrosis and ER stress through its action as a sEH inhibitor, we used a second sEH inhibitor with a different structure. Wild-type mice were treated with a second sEH inhibitor, *trans*-4-{4-[3-(4-trifluoromethoxy-phenyl)-ureido]-cyclohexyloxy}-benzoic acid (*t*-TUCB). Blood levels of the compound were determined using the procedure described above for TPPU and found to be 440 ± 36 nM midway through the experiment (2.5 week time point) and 481 ± 23 nM at the end (5 week time point.) The *t*-TUCB treated animals displayed a roughly 25 percent reduction in collagen deposition as determined by picosirius red staining (Figure 6A and B).

Quantification by LC-MS/MS revealed that the total tissue hydroxyproline levels in the livers from *t*-TUCB treated animals were not statistically different from either the Control group or the CCl_4-only group (P-value > 0.05) (Figure 6C). To further test the involvement of the sEH, C57BL mice with a disruption in the gene for sEH were treated with CCl_4, TPPU, or both. The hydroxyproline levels in the livers of the CCl_4-treated Null animals were not statistically different (P-value > 0.05) than the Null Control group, wild-type control, or the wild-type CCl_4-only group (Figure 6C). However, the CCl_4-treated Null animals displayed significantly less (P-value < 0.05) collagen deposition as judged by picosirius red staining, comparable to the CCl_4+*t*-TUCB group (Figure 6A and B). The Null +CCl_4+TPPU group did not show significant differences (P-value > 0.05) in the hydroxyproline levels or the collagen deposition from the Null+CCl_4 group (Figure 6).

Discussion

In this study, the inhibition of sEH, the major route of metabolism for EpFA such as the EETs, resulted in a dramatic attenuation of many markers of liver fibrosis and ER stress associated with CCl_4 treatment. TPPU has an IC_{50} of 8.3 nM when assayed with the recombinant murine enzyme and cyano(2-methoxynaphthalen-6-yl)methyl(3-phenyloxiran-2-yl)methyl carbonate (CMNPC) as the substrate (Liu *et al.*, 2013), so the plasma levels of TPPU in this study were well above the concentration required to inhibit the enzyme. TPPU treatment not only altered collagen density, but also the composition of the ECM, reducing collagen deposition and collagen 1a2 and 3a1 mRNA expression in the CCl_4+TPPU group compared to the CCl_4-only group. These changes were accompanied by dramatic shifts in MMP activity and expression, although TPPU did not alter the upregulation of TIMP-2 observed in the CCl_4-only group. Taken together, the decrease in collagen deposition and differences in expression patterns of collagen isoforms and MMPs between the CCl_4+TPPU and CCl_4-only groups indicate that the ECM in the CCl_4+TPPU

group more closely resemble the control tissue. The shifts in MMP expression, especially, may have implications for tissue regeneration and recovery from fibrosis, where there is evidence that sEH plays a role. A recent study reported that treatment with a sEH inhibitor increased liver to body weight ratio after partial hepatectomy and sEH null mice displayed accelerated skin wound healing (Panigrahy *et al.*, 2013). Regenerative physiological processes like these are facilitated by ECM reorganization and construction, which require changes in MMP activity.

Our zymography yielded unexpected results. We detected a modest increase in pro-MMP-9 activity in the CCl_4-only group that was attenuated by TPPU treatment and no change in MMP-2 activity. Upregulation of MMP-9 expression and increased MMP-9 activity have been associated with the progression of liver fibrosis in both human and rodent (Kurzepa *et al*, 2014), and therefore reduction in MMP-9 activity should attenuate pro-fibrotic matrix remolding. By far, the most striking result was the dramatic increase in gelatinase activity in the 45–54 kDa range in the TPPU+CCl_4 group relative to all other groups. This molecular weight range corresponds to active MMP-1a (Balbin *et al.*, 2001). MMP-1a, first characterized in 2001, has been primarily investigated in the context of cancer, where knockout of the gene causes an increase in tumor growth and angiogenesis in a Lewis lung carcinoma mouse model (Fanjul-Fernández, et al. 2013; Foley *et al*., 2014). The role that MMP-1a may play in the observed anti-fibrotic effects of sEH inhibition is currently under investigation.

While the change in most inflammatory cytokines and growth factors did not pass the statistical test, TGFβ1 was substantially reduced in the CCl_4+TPPU group relative to the CCl_4-only group. TGFβ impacts fibrosis through multiple mechanisms including the modulation of MMP and TIMP expression and the stimulation of the production of matrix components such as the collagens and integrin α2 (Baghy *et al.*, 2012). The reduction of TGFβ in the TPPU+CCl_4 relative to the CCl_4-only group is further indirect evidence of the changes to the ECM elicited by sEH inhibition. Our observation parallels a result obtained in a rat diabetic model of kidney fibrosis, in which the elevation of TGFβ in the fibrotic kidney was reduced by administration of a sEH inhibitor (Elmarakby *et al.*, 2013). It should be noted that these mRNA expression data may not reflect hepatic protein or enzymatic activity levels.

Because sEH inhibition changes oxylipid metabolism, we examined plasma levels of EpFA. Despite a high degree of variation, 12-HETE was identified as a potential marker of CCl_4-induced liver fibrosis. 12-HETE has been previously identified in the sputum of patients with cystic fibrosis (Yang *et al.*, 2012). It is generated by 12-lipoxygenase (12-LOX), which has been studied in the context of cardiac hypertrophy and fibrosis. Overexpression of 12-LOX in rat cardiac fibroblasts results in increased collagen and fibronectin secretion (Wen *et al.*, 2003).

Recent studies provided evidence that ER stress can affect production of the extracellular matrix and consequently the progression of fibrotic diseases (Mollica *et al.*, 2011; Lenna and Trojanowska, 2012; Tanjore *et al.*, 2012), including hepatic fibrosis that results from the injection of CCl_4 (Ji *et al.*, 2011; Lee *et al.*, 2011; Jin *et al.*, 2013). In a nonalcoholic

steatohepatitis methionine-choline-deficient diet-induced model, liver fibrosis correlated with the increased expression of BiP and activation of caspases 12 and 7 (Mu *et al.*, 2009). Moreover, soluble mediators secreted mainly by the ER in steatotic hepatocytes and activated Kupffer cells mediate their trans-differentiation into myofibroblasts, which secrete fibrogenic cytokines and matrix components that trigger fibrosis (Yang *et al.*, 2007; Mollica *et al.*, 2011). Indeed, fibrogenic activity in hepatic stellate cells increases upon induction of ER stress (Hernandez-Gea *et al.*, 2013). Recently, we identified sEH as a regulator of ER stress in murine models of high fat diet-induced ER stress. sEH deficiency or pharmacological inhibition attenuated high fat diet-induced ER stress in liver and adipose tissue (Bettaieb *et al.*, 2013). In addition, sEH inhibition attenuates high fat diet-induced hepatic steatosis due to reduced inflammatory state (Liu *et al.*). sEH inhibition also prevents renal fibrosis through reduction of TGF-β and fibronectin expression in diabetic spontaneously hypertensive rats (Elmarakby *et al.*, 2013). Together, these data suggest that sEH contributes to ER stress-mediated TGF-β regulation of ECM production and trafficking. Genetic and chemical knockouts of the sEH as well as administration of EpFA alter a diversity of pathological states generally toward improved health. In several of these situations, now including CCl_4-induced hepatic fibrosis, reduction in ER stress appears to be a common underlying mechanism.

In order to address if TPPU was targeting the sEH as its primary mechanism of reducing fibrosis and ER stress, two experimental strategies were employed. First, animals were treated with an alternative sEH inhibitor with a substantially different structure than TPPU, *t*-TUCB, which has an IC_{50} of 11 nM when assayed with the recombinant murine enzyme and CMNPC as the substrate (Liu *et al.*, 2013). Second, sEH null mice were used. Both the CCl_4+ *t*-TUCB and Null+CCl_4 groups displayed a reduction in collagen deposition compared to the CCl_4-only group, as judged by picosirius red staining. Importantly, TPPU treatment in the null background did not yield a further reduction in fibrosis. Taken together, these data indicate that TPPU is producing the observed anti-fibrotic effects through inhibition of sEH. Hopefully, a better understanding of sEH function will provide new insight into the development of hepatic fibrosis due to exposure to carbon tetrachloride and other industrial and environmental chemicals.

Supplementary Material

Refer to Web version on PubMed Central for supplementary material.

Acknowledgments

This work was supported by NIEHS grant R37 ES02710 (to B.D.H.) and NIEHS Superfund P42 ES04699 (to B.D.H.). Partial support was provided by the West Coast Comprehensive Metabolomics Resources Core NIH/NIDDK U24 DK097154 (to B.D.H.). T.R.H. is also supported by NIH T32 training grant in basic and translational cardiovascular science (T32 HL86350). Research in the F.G.H. laboratory is supported by R01DK090492. A.B is supported by K99/R00 (1K99DK100736-01). Research in the N.C. laboratory is supported by the NIH grant HL85727 and HL85844 and Veterans Administration Merit Review Grant I01 BX000576. Imaging of αSMA was conducting using the CAMI core facility at UC Davis Center for Health and the Environment.

Abbreviations

ATF6	Activating transcription factor
BiP	Immunoglobulin-heavy-chain-binding protein
CCl_4	Carbon tetrachloride
CHOP	4 chemokine receptor 2
COX	Cyclooxygenase
ECM	Extracellular matrix
EpFA	Epoxy fatty acids
ER	Endoplasmic reticulum
JNK	Jun N-terminal kinase
LOX	Lipoxygenase
MMP	Matrix metalloprotease
PERK	PKR-like ER kinase
sEH	Soluble epoxide hydrolase
TIMP	Tissue inhibitors of metalloproteases
TPPU	1-trifluoromethoxyphenyl-3-(1-propionylpiperidin-4-yl) urea
***t*-TUCB**	*trans*-4-{4-[3-(4-trifluoromethoxy-phenyl)-ureido]-cyclohexyloxy}-benzoic acid

References

Baghy K, Iozzo RV, Kovalszky I. Decorin-TGFbeta axis in hepatic fibrosis and cirrhosis. J Histochem Cytochem. 2012; 60:262–268. [PubMed: 22260996]

Balbin M, Fueyo A, Knauper V, Lopez JM, Alvarez J, Sanchez LM, Quesada V, Bordallo J, Murphy G, Lopez-Otin C. Identification and enzymatic characterization of two diverging murine counterparts of human interstitial collagenase (MMP-1) expressed at sites of embryo implantation. J Biol Chem. 2001; 276:10253–10262. [PubMed: 11113146]

Bataller R, Brenner DA. Liver fibrosis. J Clin Invest. 2005; 115:209–218. [PubMed: 15690074]

Bettaieb A, Nagata N, AbouBechara D, Chahed S, Morisseau C, Hammock BD, Haj FG. Soluble epoxide hydrolase deficiency or inhibition attenuates diet-induced endoplasmic reticulum stress in liver and adipose tissue. J Biol Chem. 2013; 288:14189–14199. [PubMed: 23576437]

Chan CC, Lee KC, Huang YH, Chou CK, Lin HC, Lee FY. Regulation by resveratrol of the cellular factors mediating liver damage and regeneration after acute toxic liver injury. J Gastroenterol Hepatol. 2013; 29:603–613. [PubMed: 23981054]

Chiang CK, Hsu SP, Wu CT, Huang JW, Cheng HT, Chang YW, Hung KY, Wu KD, Liu SH. Endoplasmic reticulum stress implicated in the development of renal fibrosis. Mol Med. 2011; 17:1295–1305. [PubMed: 21863214]

Constandinou C, Henderson N, Iredale JP. Modeling liver fibrosis in rodents. Methods Mol Med. 2005; 117:237–250. [PubMed: 16118456]

El-Swefy S, Hassanen SI. Improvement of hepatic fibrosis by leukotriene inhibition in cholestatic rats. Ann Hepatol. 2009; 8:41–49. [PubMed: 19221533]

Elmarakby AA, Faulkner J, Pye C, Rouch K, Alhashim A, Maddipati KR, Baban B. Role of haem oxygenase in the renoprotective effects of soluble epoxide hydrolase inhibition in diabetic spontaneously hypertensive rats. Clin Sci (Lond). 2013; 125:349–359. [PubMed: 23611540]

Fanjul-Fernández M, Folgueras AR, Fueyo A, Balbín M, Suárez MF, Fernández-García MS, Shapiro SD, Freije JM, López-Otín C. Matrix metalloproteinase Mmp-1a is dispensable for normal growth and fertility in mice and promotes lung cancer progression by modulating inflammatory responses. J Biol Chem. 2013; 288:14647–14656. [PubMed: 23548910]

Foley CJ, Fanjul-Fernández M, Bohm A, Nguyen N, Agarwal A, Austin K, Koukos G, Covic L, López-Otín C, Kuliopulos A. Matrix metalloprotease 1a deficiency suppresses tumor growth and angiogenesis. Oncogene. 2014; 33:2264–2272. [PubMed: 23708660]

Funk CD. Prostaglandins and leukotrienes: advances in eicosanoid biology. Science. 2001; 294:1871–1875. [PubMed: 11729303]

Hernandez-Gea V, Friedman SL. Pathogenesis of liver fibrosis. Annu Rev Pathol. 2011; 6:425–456. [PubMed: 21073339]

Hernandez-Gea V, Hilscher M, Rozenfeld R, Lim MP, Nieto N, Werner S, Devi LA, Friedman SL. Endoplasmic reticulum stress induces fibrogenic activity in hepatic stellate cells through autophagy. J Hepatol. 2013; 59:98–104. [PubMed: 23485523]

Hong IH, Park SJ, Goo MJ, Lee HR, Park JK, Ki MR, Kim SH, Lee EM, Kim AY, Jeong KS. JNK1 and JNK2 regulate alpha-SMA in hepatic stellate cells during CCl_4-induced fibrosis in the rat liver. Pathol Int. 2013; 63:483–491. [PubMed: 24134609]

Horrillo R, Planaguma A, Gonzalez-Periz A, Ferre N, Titos E, Miquel R, Lopez-Parra M, Masferrer JL, Arroyo V, Claria J. Comparative protection against liver inflammation and fibrosis by a selective cyclooxygenase-2 inhibitor and a nonredox-type 5-lipoxygenase inhibitor. J Pharmacol Exp Ther. 2007; 323:778–786. [PubMed: 17766677]

Hotamisligil GS. Endoplasmic reticulum stress and the inflammatory basis of metabolic disease. Cell. 2010; 140:900–917. [PubMed: 20303879]

Hui AY, Leung WK, Chan HL, Chan FK, Go MY, Chan KK, Tang BD, Chu ES, Sung JJ. Effect of celecoxib on experimental liver fibrosis in rat. Liver Int. 2006; 26:125–136. [PubMed: 16420518]

Hummasti S, Hotamisligil GS. Endoplasmic reticulum stress and inflammation in obesity and diabetes. Circ Res. 2010; 107:579–591. [PubMed: 20814028]

Hwang SH, Tsai HJ, Liu JY, Morisseau C, Hammock BD. Orally bioavailable potent soluble epoxide hydrolase inhibitors. J Med Chem. 2007; 50:3825–3840. [PubMed: 17616115]

Iredale JP. Models of liver fibrosis: exploring the dynamic nature of inflammation and repair in a solid organ. J Clin Invest. 2007; 117:539–548. [PubMed: 17332881]

Iyer A, Kauter K, Alam MA, Hwang SH, Morisseau C, Hammock BD, Brown L. Pharmacological inhibition of soluble epoxide hydrolase ameliorates diet-induced metabolic syndrome in rats. Exp Diabetes Res. 2012; 2012:758614–758624. [PubMed: 22007192]

Ji C, Kaplowitz N, Lau MY, Kao E, Petrovic LM, Lee AS. Liver-specific loss of glucose-regulated protein 78 perturbs the unfolded protein response and exacerbates a spectrum of liver diseases in mice. Hepatology. 2011; 54:229–239. [PubMed: 21503947]

Jin CF, Li B, Lin SM, Yadav RK, Kim HR, Chae HJ. Mechanism of the inhibitory effects of eucommia ulmoides oliv. cortex extracts (EUCE) in the CCl_4-induced acute liver lipid accumulation in rats. Int J Endocrinol. 2013; 2013:751854–751864. [PubMed: 24027582]

Kaufman RJ, Scheuner D, Schroder M, Shen X, Lee K, Liu CY, Arnold SM. The unfolded protein response in nutrient sensing and differentiation. Nat Rev Mol Cell Biol. 2002; 3:411–421. [PubMed: 12042763]

Kim SM, Park KC, Kim HG, Han SJ. Effect of selective cyclooxygenase-2 inhibitor meloxicam on liver fibrosis in rats with ligated common bile ducts. Hepatol Res. 2008; 38:800–809. [PubMed: 18462380]

Kindt E, Gueneva-Boucheva K, Rekhter MD, Humphries J, Hallak H. Determination of hydroxyproline in plasma and tissue using electrospray mass spectrometry. J Pharm Biomed Anal. 2003; 33:1081–1092. [PubMed: 14656599]

Kompa AR, Wang BH, Xu G, Zhang Y, Ho PY, Eisennagel S, Thalji RK, Marino JP Jr, Kelly DJ, Behm DJ, Krum H. Soluble epoxide hydrolase inhibition exerts beneficial anti-remodeling actions post-myocardial infarction. Int J Cardiol. 2013; 167:210–219. [PubMed: 22236509]

Kurzepa J, Madro A, Czechowska G, Kurzepa J, Celinski K, Kazmierak W, Slomka M. Role of MMP-2 and MMP-9 and their natural inhibitors in liver fibrosis, chronic pancreatitis and non-specific inflammatory bowel diseases. Hepatobiliary Pancreat Dis Int. 2014; 13:570–579. [PubMed: 25475858]

Lee GH, Bhandary B, Lee EM, Park JK, Jeong KS, Kim IK, Kim HR, Chae HJ. The roles of ER stress and P450 2E1 in CCl(4)-induced steatosis. Int J Biochem Cell Biol. 2011; 43:1469–1482. [PubMed: 21722752]

Lenna S, Trojanowska M. The role of endoplasmic reticulum stress and the unfolded protein response in fibrosis. Curr Opin Rheumatol. 2012; 24:663–668. [PubMed: 22918530]

Lewis MD, Roberts BJ. Role of CYP2E1 activity in endoplasmic reticulum ubiquitination, proteasome association, and the unfolded protein response. Arch Biochem Biophys. 2005; 436:237–245. [PubMed: 15797236]

Li J, Carroll MA, Chander PN, Falck JR, Sangras B, Stier CT. Soluble epoxide hydrolase inhibitor, AUDA, prevents early salt-sensitive hypertension. Front Biosci. 2008; 13:3480–3487. [PubMed: 18508449]

Liu JY, Lin YP, Qiu H, Morisseau C, Rose TE, Hwang SH, Chiamvimonvat N, Hammock BD. Substituted phenyl groups improve the pharmacokinetic profile and anti-inflammatory effect of urea-based soluble epoxide hydrolase inhibitors in murine models. Eur J Pharm Sci. 2013; 48:619–627. [PubMed: 23291046]

Liu Y, Dang H, Li D, Pang W, Hammock BD, Zhu Y. Inhibition of soluble epoxide hydrolase attenuates high-fat-diet-induced hepatic steatosis by reduced systemic inflammatory status in mice. PloS One. 2012; 7:e39165. [PubMed: 22720061]

Luria A, Weldon SM, Kabcenell AK, Ingraham RH, Matera D, Jiang H, Gill R, Morisseau C, Newman JW, Hammock BD. Compensatory mechanism for homeostatic blood pressure regulation in Ephx2 gene-disrupted mice. J Biol Chem. 2007; 282:2891–2898. [PubMed: 17135253]

Ma JQ, Ding J, Zhang L, Liu CM. Hepatoprotective properties of sesamin against CCl induced oxidative stress-mediated apoptosis in mice via JNK pathway. Food Chem Toxicol. 2014; 64:41–48. [PubMed: 24287204]

Martino MB, Jones L, Brighton B, Ehre C, Abdulah L, Davis CW, Ron D, O'Neal WK, Ribeiro CM. The ER stress transducer IRE1beta is required for airway epithelial mucin production. Mucosal Immunol. 2013; 6:639–654. [PubMed: 23168839]

Mollica MP, Lionetti L, Putti R, Cavaliere G, Gaita M, Barletta A. From chronic overfeeding to hepatic injury: role of endoplasmic reticulum stress and inflammation. Nutr Metab Cardiovasc Dis. 2011; 21:222–230. [PubMed: 21277757]

Moran-Salvador E, Titos E, Rius B, Gonzalez-Periz A, Garcia-Alonso V, Lopez-Vicario C, Miquel R, Barak Y, Arroyo V, Claria J. Cell-specific PPARgamma deficiency establishes anti-inflammatory and anti-fibrogenic properties for this nuclear receptor in non-parenchymal liver cells. J Hepatol. 2013; 59:1045–1053. [PubMed: 23831119]

Morisseau C, Hammock BD. Impact of soluble epoxide hydrolase and epoxyeicosanoids on human health. Annu Rev Pharmacol Toxicol. 2013; 53:37–58. [PubMed: 23020295]

Mu YP, Xi XH, Chen XR. Mechanism of hepatocyte regeneration inhibition in rats with liver fibrosis induced by lipogenic methionine-choline- deficient diet. Z Zhonghua Yi Xue Za Zhi. 2009; 89:3430–3436.

Ni Fhlathartaigh M, McMahon J, Reynolds R, Connolly D, Higgins E, Counihan T, Fitzgerald U. Calreticulin and other components of endoplasmic reticulum stress in rat and human inflammatory demyelination. Acta Neuropathol Commun. 2013; 1:37. [PubMed: 24252779]

Nishitoh H, Matsuzawa A, Tobiume K, Saegusa K, Takeda K, Inoue K, Hori S, Kakizuka A, Ichijo H. ASK1 is essential for endoplasmic reticulum stress-induced neuronal cell death triggered by expanded polyglutamine repeats. Genes Dev. 2002; 16:1345–1355. [PubMed: 12050113]

Panigrahy D, Kalish BT, Huang S, Bielenberg DR, Le HD, Yang J, Edin ML, Lee CR, Benny O, Mudge DK, Butterfield CE, Mammoto A, Mammoto T, Inceoglu B, Jenkins RL, Simpson MA,

Akino T, Lih FB, Tomer KB, Ingber DE, Hammock BD, Falck JR, Manthati VL, Kaipainen A, D'Amore PA, Puder M, Zeldin DC, Kieran MW. Epoxyeicosanoids promote organ and tissue regeneration. Proc Natl Acad Sci U S A. 2013; 110:13528–13533. [PubMed: 23898174]

Ron D, Walter P. Signal integration in the endoplasmic reticulum unfolded protein response. Nat Rev Mol Cell Biol. 2007; 8:519–529. [PubMed: 17565364]

Rose TE, Morisseau C, Liu JY, Inceoglu B, Jones PD, Sanborn JR, Hammock BD. 1-Aryl-3-(1-acylpiperidin-4-yl)urea inhibitors of human and murine soluble epoxide hydrolase: structure-activity relationships, pharmacokinetics, and reduction of inflammatory pain. J Med Chem. 2010; 53:7067–7075. [PubMed: 20812725]

Schroder M, Kaufman RJ. The mammalian unfolded protein response. Annu Rev Biochem. 2005; 74:739–789. [PubMed: 15952902]

Sirish P, Li N, Liu JY, Lee KS, Hwang SH, Qiu H, Zhao C, Ma SM, Lopez JE, Hammock BD, Chiamvimonvat N. Unique mechanistic insights into the beneficial effects of soluble epoxide hydrolase inhibitors in the prevention of cardiac fibrosis. Proc Natl Acad Sci U S A. 2013; 110:5618–5623. [PubMed: 23493561]

Snoek-van Beurden PA, Von den Hoff JW. Zymographic techniques for the analysis of matrix metalloproteinases and their inhibitors. Biotechniques. 2005; 38:73–83. [PubMed: 15679089]

Song BJ, Moon KH, Olsson NU, Salem N Jr. Prevention of alcoholic fatty liver and mitochondrial dysfunction in the rat by long-chain polyunsaturated fatty acids. J Hepatol. 2008; 49:262–273. [PubMed: 18571270]

Stables MJ, Gilroy DW. Old and new generation lipid mediators in acute inflammation and resolution. Prog Lipid Res. 2011; 50:35–51. [PubMed: 20655950]

Tanjore H, Blackwell TS, Lawson WE. Emerging evidence for endoplasmic reticulum stress in the pathogenesis of idiopathic pulmonary fibrosis. Am J Physiol Lung Cell Mol Physiol. 2012; 302:L721–729. [PubMed: 22287606]

Wen Y, Gu J, Peng X, Zhang G, Nadler J. Overexpression of 12-lipoxygenase and cardiac fibroblast hypertrophy. Trends Cardiovasc Med. 2003; 13:129–136. [PubMed: 12732445]

Wu D, Cederbaum AI. Inhibition of autophagy promotes CYP2E1-dependent toxicity in HepG2 cells via elevated oxidative stress, mitochondria dysfunction and activation of p38 and JNK MAPK. Redox Biol. 2013; 1:552–565. [PubMed: 24273738]

Wynn TA, Ramalingam TR. Mechanisms of fibrosis: therapeutic translation for fibrotic disease. Nat Med. 2012; 18:1028–1040. [PubMed: 22772564]

Yang J, Eiserich JP, Cross CE, Morrissey BM, Hammock BD. Metabolomic profiling of regulatory lipid mediators in sputum from adult cystic fibrosis patients. Free Radic Biol Med. 2012; 53:160–171. [PubMed: 22580336]

Yang J, Schmelzer K, Georgi K, Hammock BD. Quantitative profiling method for oxylipin metabolome by liquid chromatography electrospray ionization tandem mass spectrometry. Anal Chem. 2009; 81:8085–8093. [PubMed: 19715299]

Yang L, Jhaveri R, Huang J, Qi Y, Diehl AM. Endoplasmic reticulum stress, hepatocyte CD1d and NKT cell abnormalities in murine fatty livers. Lab Invest. 2007; 87:927–937. [PubMed: 17607300]

Yu J, Hui AY, Chu ES, Go MY, Cheung KF, Wu CW, Chan HL, Sung JJ. The anti-inflammatory effect of celecoxib does not prevent liver fibrosis in bile duct-ligated rats. Liver Int. 2009; 29:25–36. [PubMed: 18435714]

Zha BS, Zhou H. ER stress and lipid metabolism in adipocytes. Biochem Res Int. 2012; 2012:312943. [PubMed: 22400114]

Zhang K, Wang S, Malhotra J, Hassler JR, Back SH, Wang G, Chang L, Xu W, Miao H, Leonardi R, Chen YE, Jackowski S, Kaufman RJ. The unfolded protein response transducer IRE1alpha prevents ER stress-induced hepatic steatosis. EMBO J. 2011; 30:1357–1375. [PubMed: 21407177]

Zhang Y, Dong L, Yang X, Shi H, Zhang L. alpha-Linolenic acid prevents endoplasmic reticulum stress-mediated apoptosis of stearic acid lipotoxicity on primary rat hepatocytes. Lipids Health Dis. 2011; 10:81. [PubMed: 21592363]

Zinszner H, Kuroda M, Wang X, Batchvarova N, Lightfoot RT, Remotti H, Stevens JL, Ron D. CHOP is implicated in programmed cell death in response to impaired function of the endoplasmic reticulum. Genes Dev. 1998; 12:982–995. [PubMed: 9531536]

Highlights

- We administer in an inhibitor of sEH in a CCl4 murine model
- sEH inhibition reduces liver collagen deposition and pro-fibrotic gene expression
- sEH inhibition induces MMP-1a activity

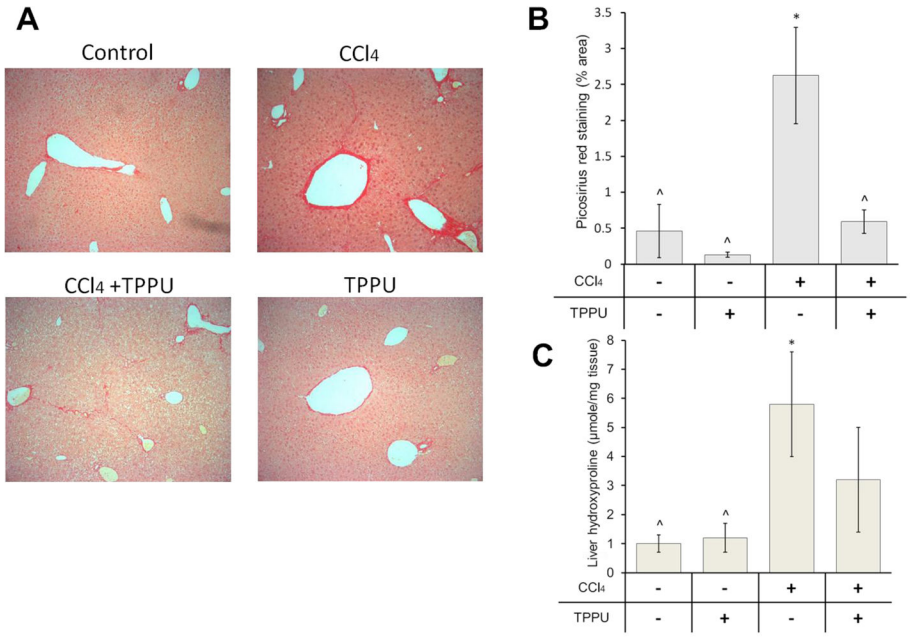

Figure 1.

TPPU attenuates collagen deposition due to CCl_4 treatment. Mice were injected (I.P.) with CCl_4 for 5 weeks as described in Materials and Methods. TPPU was administered in drinking water starting with CCl_4 treatment. A) Representative slides of liver sections stained with picosirius red (40x). B) Quantification of staining expressed in percent area. C) Quantification of hydroxyproline levels in liver tissue. Error bars represent standard error. *P-value vs. Control group < 0.05. ^ P-value vs. CCl_4-only group < 0.05. N = 6–8 animals per group.

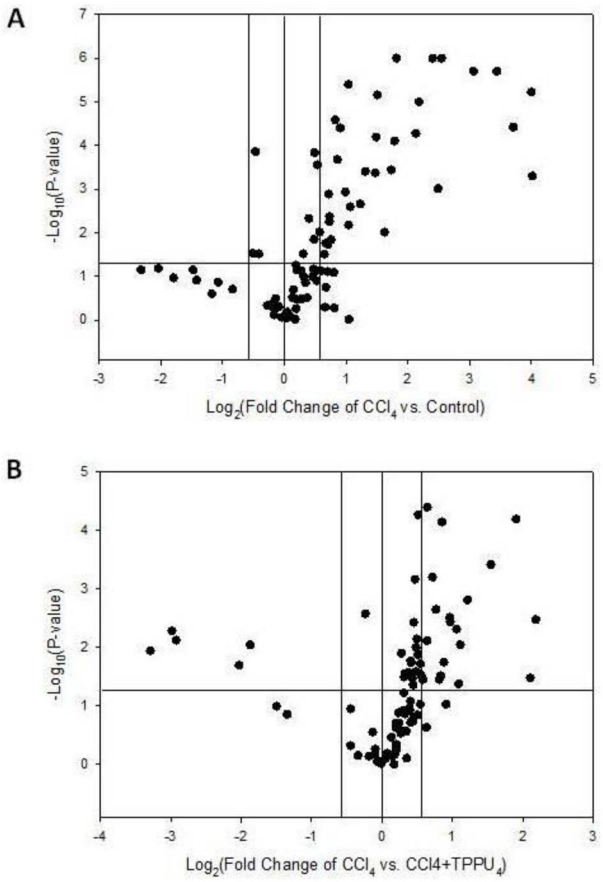

Figure 2.

TPPU treatment reduces the upregulation of pro-inflammatory and pro-fibrotic genes associated with fibrosis. PCR array analysis of hepatic tissues after 5 weeks of CCl_4 treatment. TPPU was administered in drinking water starting with CCl_4 treatment. A volcano plot of PCR array data from hepatic tissue. The log of the fold regulation of an experimental group relative to control is plotted versus the log base 10 of the P-value. A P-value of 0.05 is indicated by the horizontal line. The vertical lines on either side of the axis represent 1.5-fold induction relative to the Control group. A) The change in CCl_4-only group versus the Control group. B) The change in CCl_4 group relative to the CCl_4+TPPU group. N=6–8 animals per group. Full results in supplementary data Table S2.

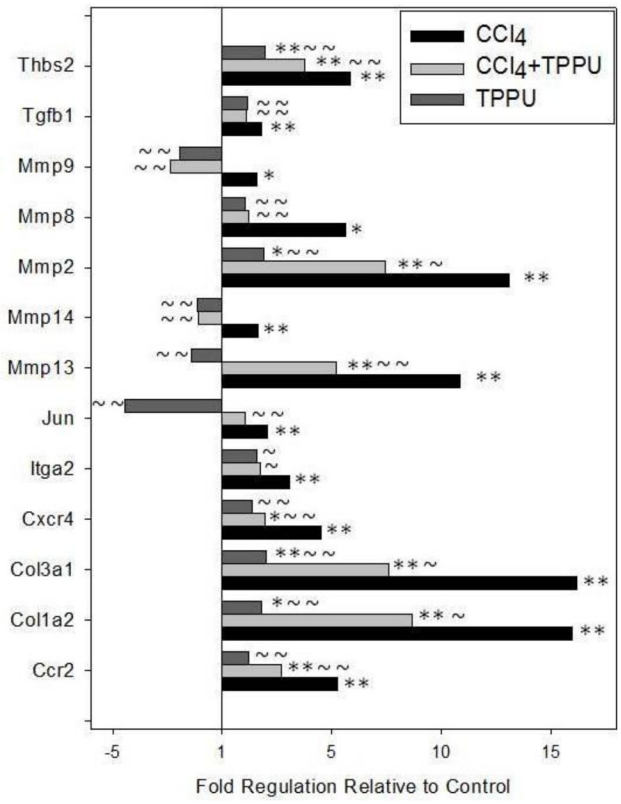

Figure 3.

TPPU treatment significantly downregulates the hepatic mRNA expression of thirteen genes compared to the CCl_4-only group. PCR array analysis of hepatic tissues after 5 weeks of CCl_4 treatment. TPPU was administered in drinking water starting with CCl_4 treatment. The genes displayed a 1.5 fold upregulation or higher in the CCl_4-only group relative to the Control group, and a concomitant downregulation in the CCl_4+TPPU versus the CCl_4-only group with a P-value of 0.05 or lower. *P-value vs. Control group ≤ 0.05; **P-value vs. Control group ≤ 0.01; ~P-value vs. CCl_4-only group ≤ 0.05; ~~P-value vs. CCl_4-only group ≤ 0.01. N=6–8 animals per group.

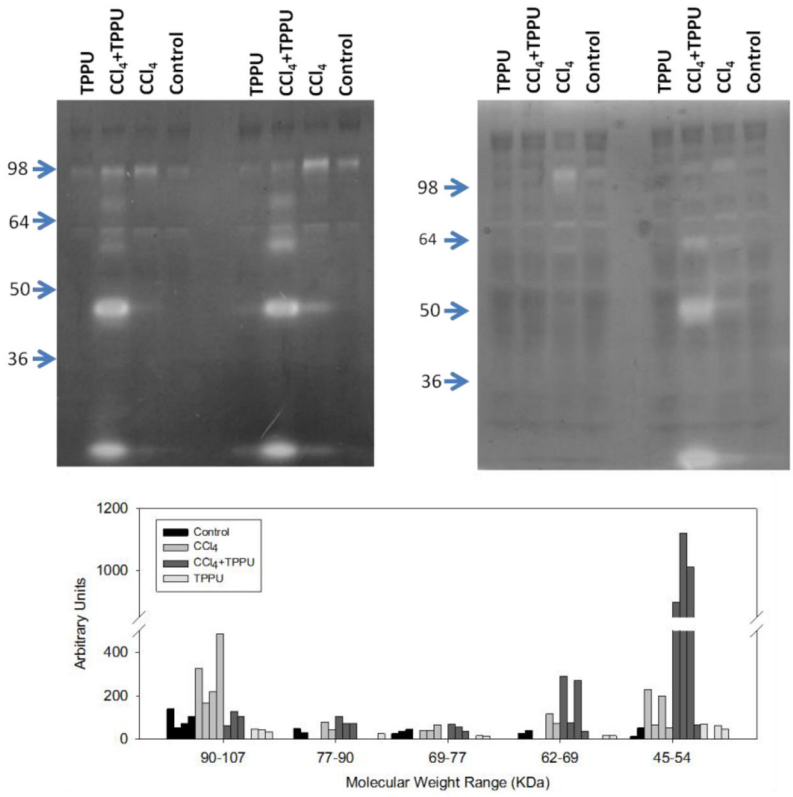

Figure 4.

TPPU modulates metalloprotease activity in hepatic tissues following CCl_4 treatment. A) Gelatin zymography. 30ug/lane of hepatic tissue lysates from control and treated groups. B) Analysis of five major bands on the gels by densitometry.

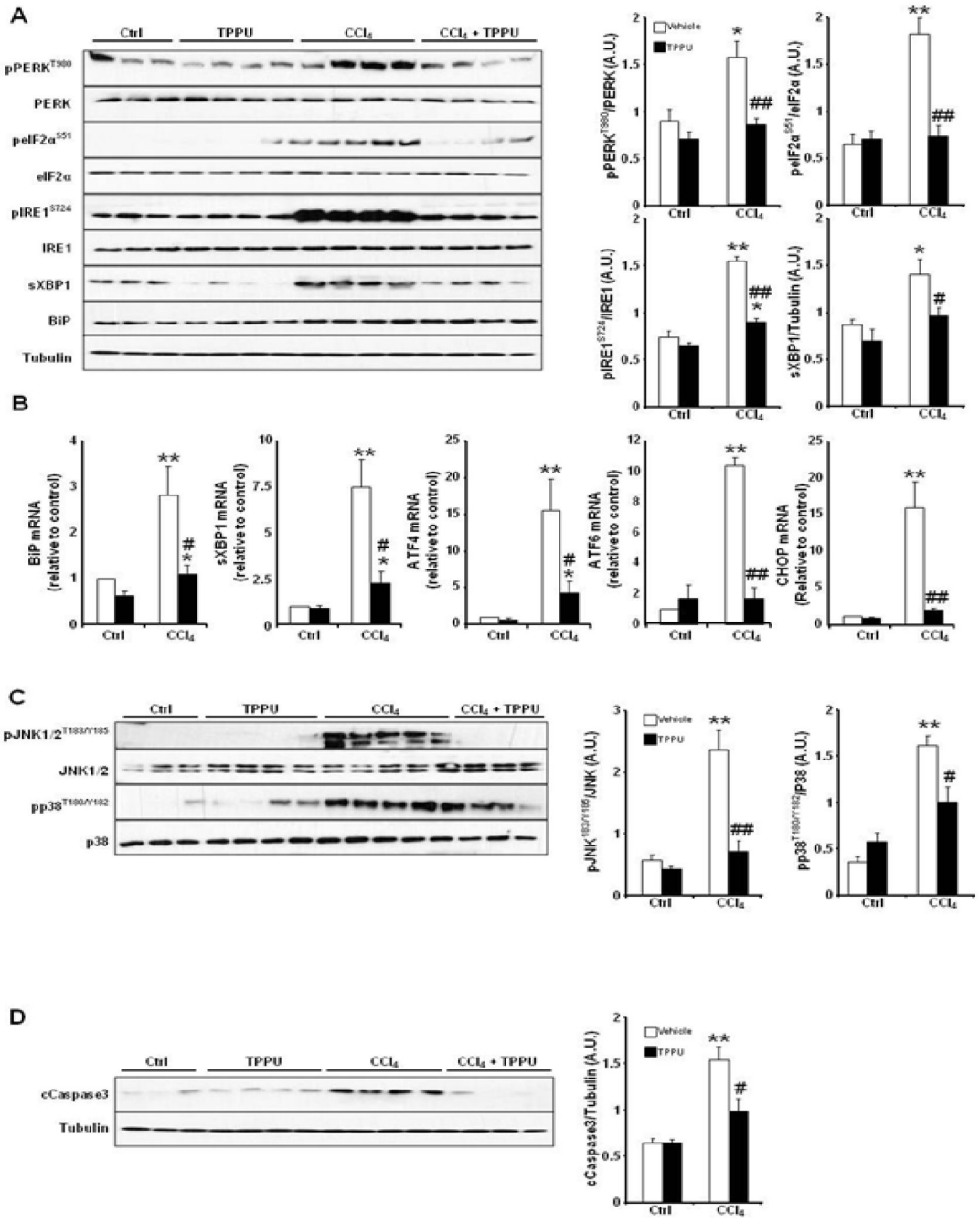

Figure 5.

sEH pharmacological inhibition mitigates CCl_4-induced ER stress *in vivo*. Mice were treated with sEH inhibitor (TPPU) or vehicle control (PEG 400) as detailed in Methods. (A) Liver lysates were immunoblotted for pPERK (Thr980), PERK, peIF2α (Ser51), eIF2α, pIRE1α (Ser724), IRE1α, spliced X-box binding protein 1 (sXBP1), BiP and Tubulin. Each lane represents a sample from a separate animal. Bar graphs represent data expressed as arbitrary units (A.U.) for pPERK/PERK, peIF2α/eIF2α, pIRE1α/IRE1α and sXBP1/Tubulin, from at least six mice and presented as means ± SEM. (B) BiP, sXBP1, ATF4, ATF6 and CHOP

mRNA from liver was measured by quantitative real-time PCR and normalized against TATA binding protein. Data represent means ± SEM of six mice. (C–D) Immunoblots of pJNK (Thr183/Tyr185), JNK, pp38 (Thr180/Tyr182), p38, cCaspase3 and Tubulin. Bar graphs represent normalized data expressed as arbitrary units (A.U.) for pJNK/JNK, pp38/p38 and Caspase3/Tubulin from at least six mice. (*) indicates significant difference between CCL_4-treated and non-treated mice, (#) indicates significant difference between TPPU-treated and non-treated mice.

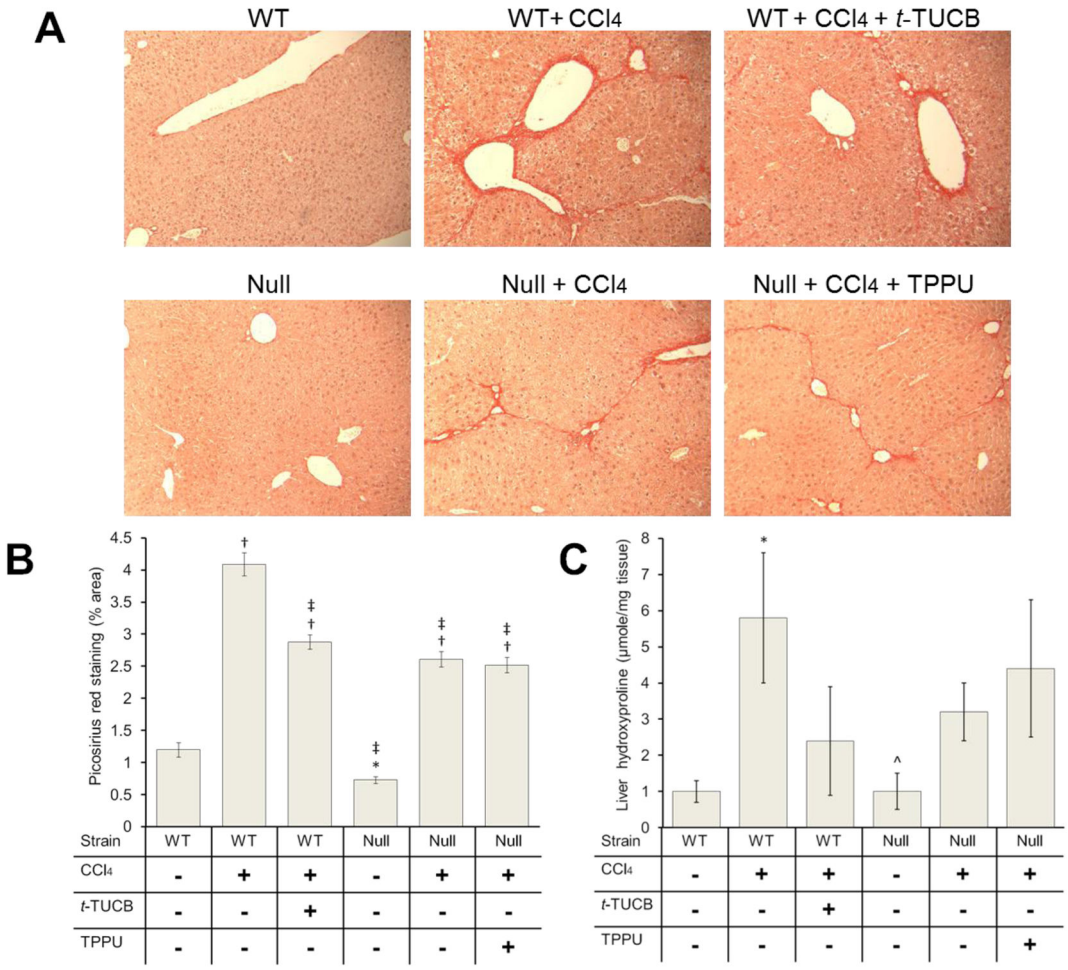

Figure 6.

t-TUCB and sEH null background attenuate collagen deposition due to CCl_4 treatment. Mice were injected (I.P.) with CCl_4 for 5 weeks as described in Materials and Methods. *t*-TUCB was administered in drinking water starting with CCl_4 treatment. C57BL mice with a sEH gene disruption (Null) were treated with CCl_4, TPPU or both. A) Representative slides of liver sections stained with picosirius red (40x). B) Quantification of staining expressed in percent area. C) Quantification of hydroxyproline levels in liver tissue. Error bars represent standard error. †P-value vs. wild-type Control group < 0.001. ‡P-value vs. wild-type CCl_4-only group < 0.001. *P-value vs. wild-type Control group < 0.05. ^ P-value vs. wild-type CCl_4-only group < 0.05. N = 6–8 animals per group.